INVITED PAPER

Prediction of Distal Arm Posture in 3-D Space From Shoulder Movements for Control of Upper Limb Prostheses

Experiments indicate that voluntary shoulder movements may be used to generate the control signals needed for operation of arms and hands that are paralyzed or artificial.

By Rahul R. Kaliki, Rahman Davoodi, and Gerald E. Loeb, *Member IEEE*

ABSTRACT | C5/C6 tetraplegic patients and transhumeral amputees may be able to use voluntary shoulder motion as command signals for a functional electrical stimulation (FES) system or a transhumeral prosthesis. Such prostheses require, at the most basic level, the control of endpoint position in three dimensions, hand orientation, and grasp. Spatiotemporal synergies exist between the proximal and distal arm joints for goal-oriented reaching movements as performed by able-bodied subjects. To fit these synergies, we utilized three-layer artificial neural networks. These networks could be used as a means for obtaining user intent information during reaching movements. We conducted reaching experiments in which subjects reached to and grasped a handle in a three-dimensional gantry. In our previous work, the three rotational angles at the shoulder were used to predict elbow flexion/extension angle during reaches on a two-dimensional plane. In this paper, we extend this model to include the two translational movements at the shoulder as inputs and an additional output of forearm pronation/supination. Counterintuitively, as the complexity of the task and the complexity of the neural network architecture increased, the performance also improved.

KEYWORDS | Artificial neural networks; control; functional electrical stimulation; motor control; prosthesis; reaching; upper limb

Manuscript received December 7, 2007; revised February 1, 2008.
The authors are with the Alfred E. Mann Institute, Department of Biomedical Engineering, University of Southern California, Los Angeles, CA 90089-1112 USA.
Digital Object Identifier: 10.1109/JPROC.2008.922591

I. INTRODUCTION

Bilateral amputations and quadriplegia are debilitating conditions in which patients are unable to perform most activities of daily living. The restoration of any functionality to these patients has been the paramount goal for many researchers. Reaching and grasping objects are obviously particularly important. Advanced mechatronic prosthetic arms and hands should provide motor capability for amputees. Functional electrical stimulation (FES) to reanimate paralyzed muscles can, in principle, restore it to spinal cord injured patients. In order to apply either technology successfully, however, there must be a source of command signals to convey to the prosthetic controller the motor intentions of the user.

Most patients who have lost arm function as a result of amputation or spinal cord injury have substantial residual voluntary control of shoulder motion. Transhumeral amputation procedures try to leave a long enough stump on which to attach the socket of the prosthesis. Most surviving quadriplegic patients have lesions at or below the C4–5 vertebral junction, leaving intact at least some of the neural circuitry required for respiratory and shoulder movements while losing some or all control of the more distal joints. The hypothesis being tested in our research is that the residual voluntary shoulder movements contain sufficient information about those intentions that they can be used as a continuous source of command signals for the prosthetic controller.

A. Potential Command Sources

Due to the limited availability of voluntarily controlled movements in high-level amputations and spinal cord injuries, many investigators have looked to the brain as a

potential source of command signals for control of reach and grasp. The complexity and invasiveness of the technology are daunting and the long-term viability of the interfaces has yet to be determined. Nevertheless, Donoghue *et al.* have implanted a human subject with a microelectrode array in the primary motor cortex and the subject has achieved control of a cursor in the two-dimensional (2-D) space of a computer monitor [1]. Nicolelis *et al.* have shown that monkeys with chronically implanted microelectrodes are able to control the trajectory of a robot arm's end effector to reach to one of eight targets in three-dimensional space [2]. But the transition from control of display cursors and robotic arms to the control of anthropomorphic limbs is not trivial. This is because many of the researchers investigating motor control from the brain have been focusing on relationships between brain activity and endpoint trajectories in space and assuming that individual joint trajectories can be derived by inverse kinematic analysis. But the upper limb is an overdetermined system in that there are more joints than necessary to express a given endpoint position and orientation. This was first described by Bernstein in 1967 as the "redundancy problem" [3]. These "extra" degrees of freedom (DOFs) are important, of course, in the interaction of the hand with objects, e.g., in orienting the hand and controlling the fingers to grasp objects with different sizes, shapes, and orientations. It remains to be determined if cortical neural signals can be used to provide such control without becoming an undue burden on the user.

Recently, some investigators have developed FES systems that utilize the voluntary movements at the shoulder of these patients as control signals. One such FES system is the FreeHand system, which utilizes the residual voluntary control of the protraction/retraction of the contralateral shoulder to control the opening and closing of a hand [4]. The dependence on contralateral shoulder movements makes it unsuitable for extension to bimanual tasks and deprives users of the proprioceptive feedback that might be derived from the interaction of the command signals with the actual arm being moved. This system, while a little awkward in its method of control, is able to restore grasping function but does not lend itself to control of the equally important functionality of reaching.

Kilgore *et al.* have designed and implanted a myoelectric-based FES controller that restored reaching and grasping function [5]. Myoelectric signals related to the activities of functional muscles still under voluntary control are used as commands for individual degrees of freedom through FES. Implanted patients regained the ability to control various degrees of freedom and were able to accomplish some activities of daily living, such as eating and drinking. This method is a great improvement in terms of functionality for paraplegic patients, but the number of controlled outputs is limited by the number of viable voluntary muscles available. If some of the voluntary muscle groups were involved in other functions required by the patient, then the muscle group could not be used as a reliable command source.

A prosthesis that relies on command sources unrelated to natural reaching movements forces the user to learn unnatural reaching control strategies. Such a system could require ungainly and cumbersome movements to restore functionality. As described here, it seems desirable to extract command signals from the natural movements of the ipsilateral shoulder that the patient spent a lifetime learning before incurring injury and disability.

B. Prior Research on Ipsilateral Shoulder Control

Popovic *et al.* [6]–[8] have developed various synergy-based upper limb neuroprosthetic controllers that predicted elbow flexion/extension from shoulder flexion/extension based on simple scaling rules, through inductive learning, and from training a radial basis function network. In the latter experiment, synergy models were trained with joint acceleration data recorded from able-bodied subjects while executing a sequence of movements: reaching and grasping an object in a plane, bringing the object to the mouth, returning the object to its previous position, and returning the hand back to the initial position. Each network was trained on data for sequences of movements to one target location. The investigators found that the networks were able to predict reaches to targets located distally to the trained target reach but found that the network was unable to predict reaches to targets located laterally to the trained target reach. This indicated that the synergy rules changed across the two-dimensional workspace. Therefore, the user would need to manually select among several synergy rules based on where he or she wanted to reach. While some reaching motion could be restored to these subjects, having to switch manually between synergy rules would become cumbersome during everyday activities, especially if the user wanted to make movements across the boundaries of these regions.

In contrast to Popovic *et al.*, we hypothesize that all three degrees of freedom at the shoulder might contribute useful information that would generalize better over the whole workspace, thus eliminating the need for manual switching. Furthermore, our initial studies suggested that the spatiotemporal relationships between joint angles are relatively stable and therefore more likely to result in a user-controllable system as compared to joint velocity and joint acceleration relationships. Finally, as opposed to training synergy models with data from only a single target location, we wanted to use a set of reaches to a wide range of target locations in order to account for variations in the reaching strategy across the workspace. To test these hypotheses, we trained an adaptive neural network (ANN) to predict the elbow joint angle from the three rotational angles of the shoulder joint [9].

An experimental workspace was designed such that hand position was kept in a horizontal plane during each reach (similar to Popovic *et al.*). Sixteen rectangular-shaped

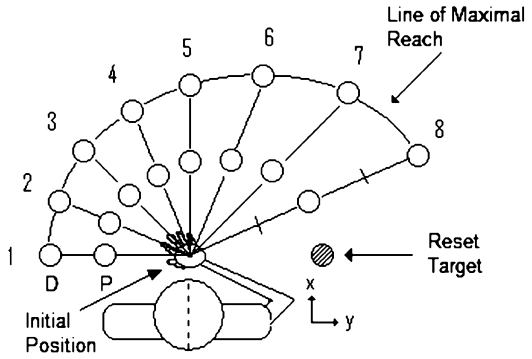

Fig. 1. *A schematic drawing of the two-dimensional workspace used in previous 2-D point-to-point reaching experiment.*

targets were placed in two concentric arcs on a pegboard as shown in Fig. 1. The distal target set was distributed on a circular arc at the maximal reach of the subject while the proximal target set was placed at the midpoint between the distal target set and the initial position. The subject was asked to make self-paced reaches from the initial position to and from the target position. Shoulder and elbow joint angles were recorded during eight trials of reaches to each of the 16 targets.

As previously discussed, the shape and orientation of the shoulder/elbow angle synergies varied greatly across the workspace [Fig. 2(a)], but in certain areas of the workspace, there were subsets of reaches that exhibited similar spatiotemporal synergies [Fig. 2(b)]. We hypothesized that the ANN might produce better results if trained only on one representative reach from each such subset, thereby avoiding overtraining on similar targets in large subsets at the expense of accuracy on the more individualized targets. To examine this supposition, we trained the ANN with incrementally added target reaching data. Target reaches were added to the training set based on the ANN's performance on the last training set. The target reach that was predicted the worst was added to the training set, and this process was continued iteratively until all the targets were added. We found that the error reached a minimum when we incorporated training data from 11 of the 16 targets. The correlation between the predicted elbow angle and the recorded angle on the validation set was 0.99. Interestingly, seven of these targets were from the distal set, indicating that the reaches to the distal targets allowed the ANN to predict reaches in the proximal set accurately, apparently because the corresponding synergies between proximal and distal targets were just scaled versions of each other.

This previous study provided the methodology and rationale for our present study of reaching to targets distributed in three dimensions, a necessary goal for most practical applications of the proposed command scheme. Furthermore, we tested whether including additional inputs (related to shoulder translation) improves the prediction of the elbow angle and whether the prediction of an additional output, forearm pronation/supination, degrades the performance of the ANN models.

II. METHODS

A. Target Locations

We constructed a large robotic gantry (Parker Hannifin, Co.) to automate the presentation of targets in the three-dimensional (3-D) workspace of the arm. The computer-controlled gantry was able to reach anywhere in a $(2 \times 1 \times 1\ \mathrm{m}^3$ workspace Fig. 3). Subjects were instructed to reach and grasp firmly a cylindrical, vertically oriented handle on the working end of the gantry arm.

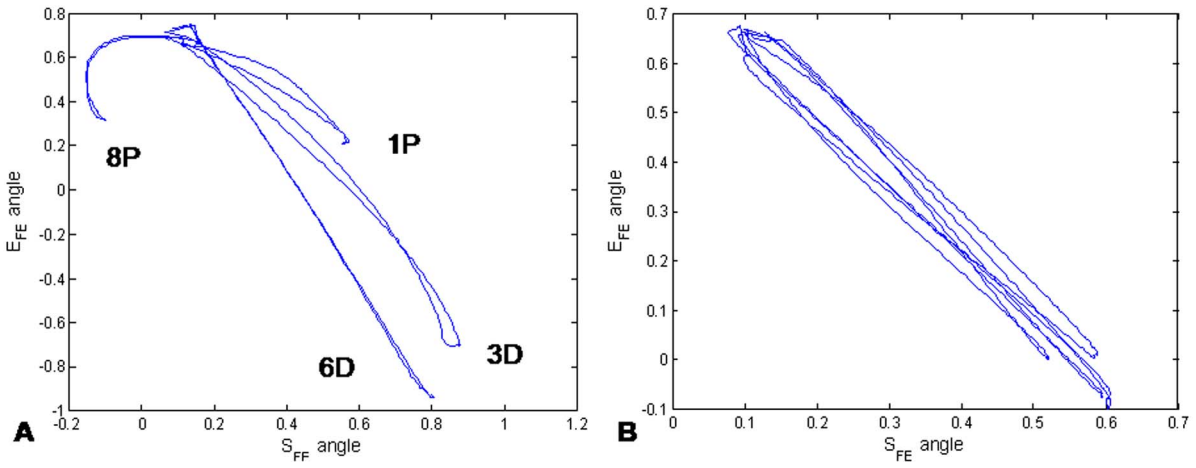

Fig. 2. *Example of shoulder/elbow synergies of target reaches in Fig. 2. (a) Shoulder/elbow joint synergies of target reaches 1P, 8P, 3-D, and 6D. (b) Shoulder/elbow joint synergies of target reaches 2-5P. Clearly there is a cluster of synergies for* E_{FE} *versus* S_{FE} *synergies.*

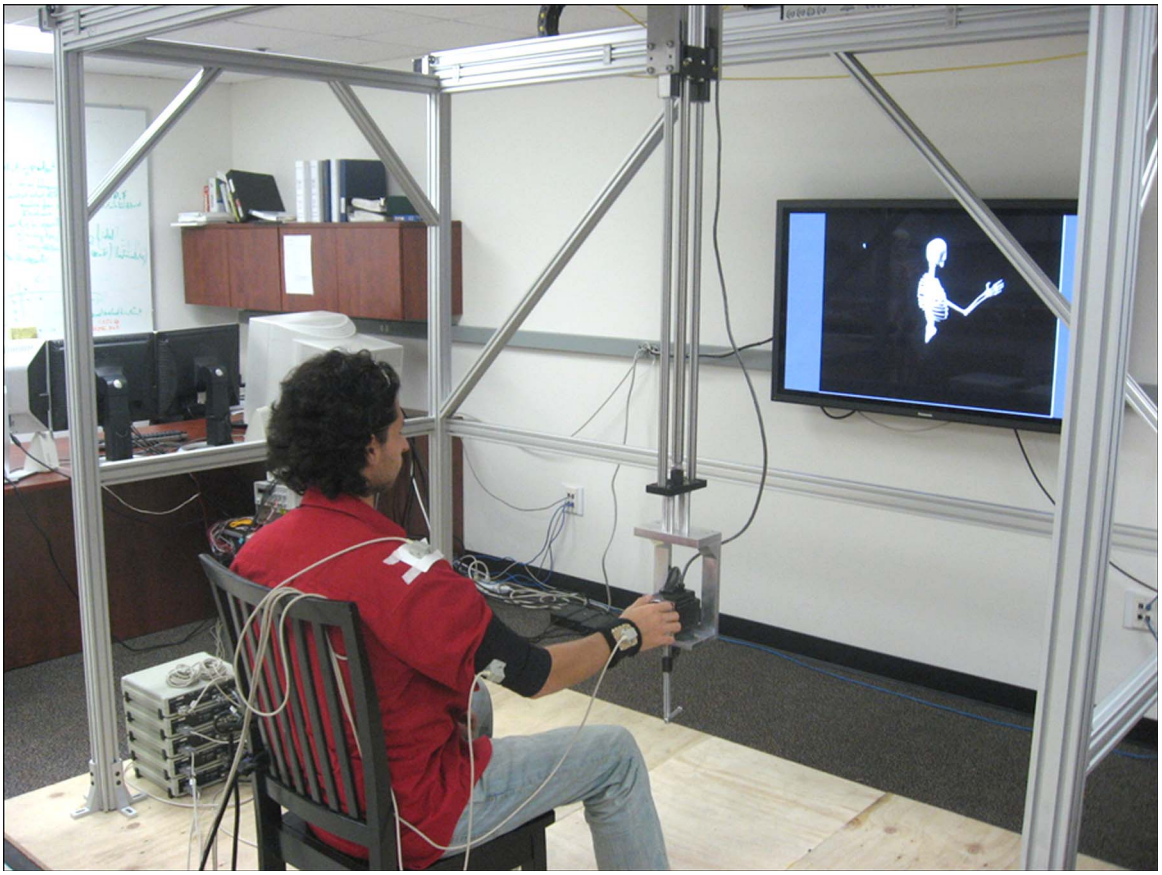

Fig. 3. ***Robotic gantry used to present targets to a subject in 3-D extrapersonal space.***

Prior to experimentation, target locations were tailored to the subject's physical measurements. Target locations were expressed in shoulder-centric spherical coordinates: α, β, and f (corresponding to the fraction of the subject's entire arm length). Measurements were taken of the subject's upper (L_1) and lower arm (L_2) segments, as well as the height of the subject's line of sight above the shoulder center of rotation (L_3) to constrain the target locations and tailor them to the subject (Fig. 3). We first defined a set of targets in the X–Z plane, which was then rotated about the z-axis to produce target locations in three dimensions. We then applied the constraints to the target set to ensure that all the targets were in a reasonable working space. L_3 and L_1 limited the maximum and minimum height of targets in the y-direction, respectively. To ensure the safety of the subject during experimentation, we kept the subject's head and body outside of the reachable area of the gantry arm. This limited the location of the front-most targets in our workspace. The distance between the front-most possible target and the shoulder center of rotation along the x-axis was measured (L_4) and was used to determine the minimum angle of α at the subject's maximal reach $(f = 1.0)$ in the two-dimensional plane. When the upper arm crosses the sagittal plane at shoulder joint $(\alpha \geq 90^\circ)$, the maximal reach length is no longer equivalent to the subject's arm length due to the restriction of movement as the humerus makes contact with the torso. In order to reduce undesirable contributions from the trunk in this area of the workspace, the line of maximal reach was approximated by fixing the humerus position at $\alpha = 90^\circ$ and bending the elbow from 0° to 90°. Intervals between targets in the α-direction were determined by the difference in the first target alpha subtracted from the final target α divided by the number of desired targets at the line of maximal reach. For this experiment, we had eight targets along the line of maximal reach $(f = 1.0)$. For all other values of f, targets were placed at that radius with the same angular interval between targets as previously determined. Once all the targets locations in the X–Z plane were determined, the plane was then rotated about the z-axis from $\beta = 90^\circ$ to $\beta = -90^\circ$. Targets that were below the length of the upper arm segment (L_1) in the y-direction or were at a height greater than the line of sight (L_3) were removed from the target set. The angular interval between targets in the β-direction was 10°.

An adult male volunteered to perform reaching experiments. His physical measurements were $L_1 = 11.5$ in, $L_2 = 14.5$ in, and $L_3 = 6.5$ in. The fraction of maximal

reach f was varied from 0.5 to 1.0, and this resulted in an experimental workspace that included 186 target locations (Fig. 5). Once the target locations were determined, they were presented to the subject in randomized order by the gantry control software.

B. Data Acquisition

The subject was asked to sit in a high-back chair, and elastic restraints were secured around the subject's torso and underneath his arms to limit contributions from the subject's trunk during movement. Additionally, we restricted the subject's wrist movements by bracing the subject's wrist with a semirigid brace. In order to record the subject's joint angles during experimentation, a Flock of Birds (Ascension Technologies Corp., Burlington, VA) motion-capturing system was used with a sample frequency of 100 Hz. Each Flock of Birds sensor measured position and orientation (measured in rotation matrices) with respect to a transmitter. Sensors were placed on the shoulder (over the Acromion) and humerus and over the wrist brace (at the distal end of radius). The transmitter was placed between the subject's knees on the chair. The Flock of Birds system was calibrated to the subject prior to experimentation. Clinically, meaningfully Euler angles were derived from the rotation matrices (Euler rotations in *X-Z-Y* order about the moving axes). The calculated shoulder joint angles were shoulder abduction/adduction (S_{ABAD}), the angles about the *x*-axis of the fixed reference frame (Fig. 5); shoulder flexion/extension (S_{FE}), the angle about the *z*-axis of the moving frame; and internal external rotation (S_{IER}), the angle about the *y*-axis of the moving frame. The other recorded angles were sternoclavicular depression/elevation (SC_{DE}), sternoclavicular protraction/retraction (SC_{PR}), elbow flexion/extension (E_{FE}), and forearm pronation/supination (F_{PS}). These values along with the original rotation matrices and the location of targets were recorded in a synchronized manner by the experiment control software.

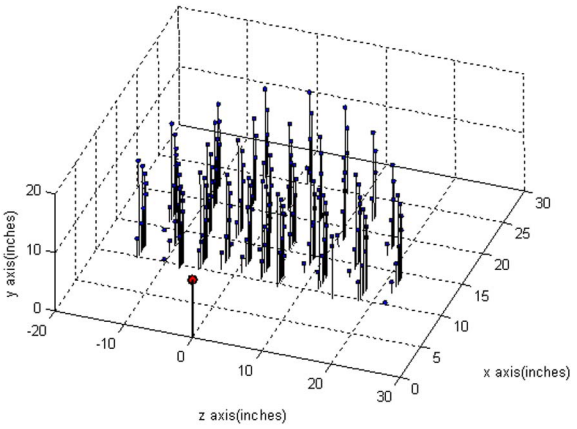

Fig. 5. *A stem plot of all the locations of the targets in extrapersonal space (blue). The shoulder center of rotation is shown in red.*

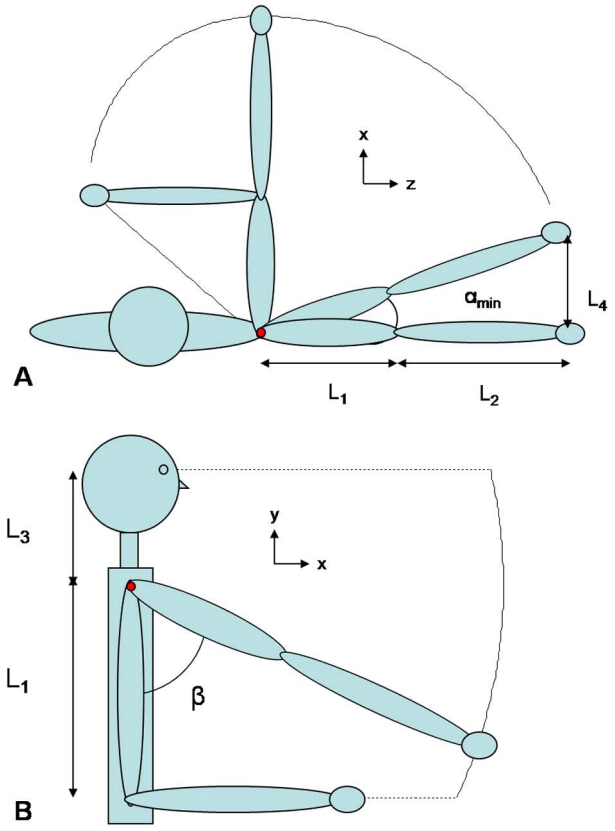

Fig. 4. *(a) Top-down view of the 2-D workspace boundary. The angle α is shown as well as significant physical measurements taken of the subject. This plane is rotated about the z-axis. (b) Side view of the workspace. The angle β is shown as rotated from $-\pi/2$ to $\pi/2$. The solid line indicates the maximal reach of the subject and dotted lines indicated artificial boundaries created to limit the workspace.*

Once the subject was secured in the chair, we placed a lap tray over the subject's lap, which indicated the desired location of the hand's initial position. During the experiment, the subject was asked to view a display with a pair of indicator lights shown. Prior to each reach, the subject's hand was lying flat (prone) at the initial position. When the left indicator light displayed a green color, the subject was cued to grasp the vertical gantry handle. The subject was told to move at a natural pace. When the subject had properly grasped the handle, the right indicator turned green. The right indicator remained green for approximately 3–5 s. When the light turned off, the subject was cued to return to the initial position. The experiment continued until all the target locations were reached.

C. Data Preprocessing and Partitioning

After experimentation, the data was filtered offline with a 3 Hz third-order Butterworth low-pass filter. The 3 Hz filtering was necessary to remove some 4 Hz noise present

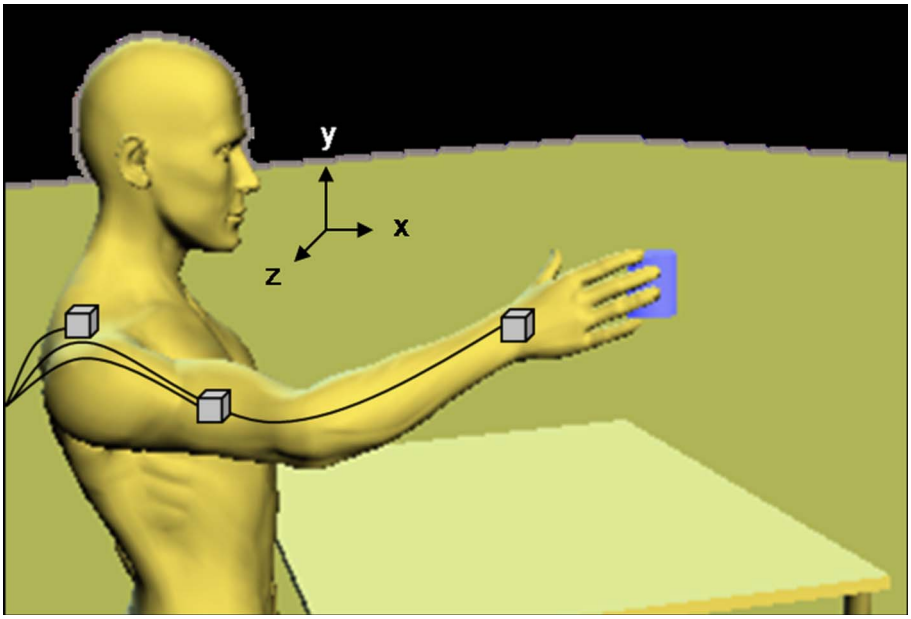

Fig. 6. *A schematic of the subject during experimentation. The locations of the Flock of Birds sensors are shown. The coordinate system used in determining the clinically meaningful Euler joint angles is shown. The recorded joint angles were shoulder abduction/adduction* ($\mathbf{S_{ABAD}}$)*, the angles about the x-axis of the fixed reference frame; shoulder flexion/extension* ($\mathbf{S_{FE}}$)*, the angle about the y-axis of the moving frame; internal external rotation* ($\mathbf{S_{IER}}$)*, the angle about the z-axis of the moving frame; sternoclavicular depression/elevation* ($\mathbf{SC_{DE}}$)*, the translation along the y-axis of the shoulder frame; sternoclavicular protraction/retraction* ($\mathbf{SC_{PR}}$)*, the translation along the x-axis of the shoulder frame; elbow flexion/extension* ($\mathbf{E_{FE}}$)*, the angle about the z-axis of the elbow frame; and forearm pronation/supination* ($\mathbf{F_{PS}}$)*, the angle about the x-axis of the elbow frame.*

in our motion-capturing hardware, as evidenced by the presence of the noise in the sensors prior to attachment to the subject. The data were then down-sampled to 8 Hz to reduce the data size and normalized by subtracting the mean from each channel and dividing by the standard deviation. Finally, data recorded during resting periods between target reaches were removed in order to limit the contribution of the initial posture to the neural network from each data set.

Prior to data partitioning, three different primary sets of target reach data were created. The first primary set (labeled "a") included data from the entire trajectories (reach plus hold period) to each of the 186 targets. In the second primary set (b), we removed all the target reach information that contained reaches in which the elbow angle while grasping the target handle was less than 10° different from the initial elbow angle. Shoulder motion accounted for most of the movement to these targets, so they were not useful for training elbow angle output. After we removed these target reaches, the data set included 146 target reaches. The third primary data set (c) included only those targets from set b that were at $f > 0.8$. This limited the data set to 50 target reaches.

Prior to ANN training, the primary data sets were divided into two sets: a secondary working set, with which the ANN was trained, and a validation set, which included novel data to evaluate the performance of the ANN. Twenty percent of the data from the primary data set were randomly chosen and set aside as the validation set. The remaining data were designated the secondary working set. From the secondary working set, 70% of the data were randomly distributed in a training set and the remaining values designated as the test set. The training set included data with which the ANN would be trained via backpropagation, and the test set was novel data used to measure the ANN's ability to generalize during ANN training.

D. Neural Network Training

Two-layer perceptron ANNs were created in NeuralWorks Predict (NeuralWare). This software employed an adaptive gradient backwards propagation algorithm to tune the weights and biases of the ANN to maximize the correlation between the model predictions and the recorded data. Hidden units had hyperbolic tangent activation functions. The output units were logistic sigmoid activation functions. Hidden layer size was determined through a cascade learning algorithm developed by Fahlman and Lebiere [10]. This algorithm adds hidden units incrementally to the hidden layer until performance on the test set is no longer improved. The software also used early stopping to prevent the ANN from overfitting and to improve generalization. Early stopping examines the performance of the ANN during training by examining its performance on the test set. If the network's performance on the test set is no longer improved, then training is stopped.

ANNs were constructed with three different input/output (I/O) relationships to examine the efficacy of different inputs and whether the addition of multiple distal angle outputs significantly degraded ANN performance. The first set of I/Os examined the ability of the three rotational joint angles at the shoulder joint (S_{FE}, S_{IER}, and S_{ABAD}) to predict the elbow angle (E_{FE}) during reaches in 3-D. ANNs trained with this set of I/Os were labeled ANN1x, where x is a place holder for the primary data set type (a, b, or c). The next set of I/Os incorporated shoulder translation movements (SC_{DE} and SC_{PR}) as inputs in addition to S_{FE}, S_{IER}, and S_{ABAD} and evaluated whether these additional inputs improved predictability of the E_{FE}. These sets of ANNs were labeled ANN2x. The third and final set of I/Os used the same input, the five DOFs at the shoulder, as the previous set but added the forearm pronation/supination (F_{PS}) in addition to E_{FE} as the outputs of the ANNs. This set of I/Os was created to examine the potential to predict F_{PS} for further study and whether predictive performance significantly degraded for prediction of the E_{FE}. The coefficient of determination (R^2) between the predicted output and recorded output was measured for all the ANNs. Any R^2 value above 0.7 was considered a strong correlation. Additionally, the root mean squared (rms) error between the predicted and recorded outputs was measured. Because the data were normalized by the standard deviation prior to training, the error is unitless.

III. RESULTS

An example of target reach data used to train neural networks is shown in Fig. 7. Table 1 shows the tabulated R^2 and rms errors for neural networks ANN1a, ANN1b, and ANN1c. Inputs to these neural networks were the three rotational angles at the shoulder while the output was the elbow angle. The errors and R^2-values are shown for each of the data sets: training, test, and validation sets. The R^2-values for each of the ANNs on the validation set were greater than 0.70 and, therefore, are considered strong correlations. The neural network trained with the distal targets ($f > 0.8$) reported the highest R^2 and lowest rms error for each of the data sets.

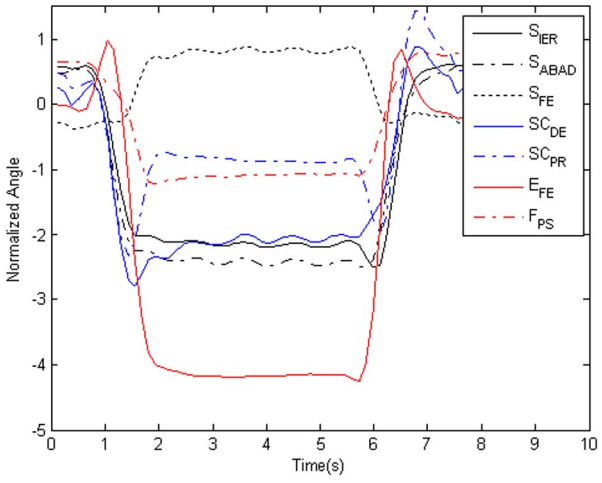

Fig. 7. *Typical example of Euler angles recorded during a reach to a target ($\alpha = 33.5°$, $\beta = 21.3°$, $f = 1.0$). The black, blue, and red plots correspond to shoulder rotational angles, shoulder translational movements, and distal arm angles.*

Table 1 Summary Data Shown for Neural Networks Trained With Three Rotational Shoulder Angles as Inputs Predicting the Elbow Angle as the Output. R^2 and Root Mean Squared Errors Shown for Train, Test, and Validation Sets

Name	Set	R^2	RMS
ANN1a	Train	0.7365	0.7093
	Test	0.7319	0.7154
	Valid	0.7026	0.7532
ANN1b	Train	0.8077	0.6735
	Test	0.7515	0.7657
	Valid	0.7751	0.7229
ANN1c	Train	0.8802	0.4657
	Test	0.8624	0.4990
	Valid	0.8406	0.5207

Table 2 summarizes the performance of neural networks ANN2a, ANN2b, and ANN2c. The inputs to these neural networks were the three rotational angles and two translational movements at the shoulder. The output was the elbow angle. The R^2-values and rms error values are tabulated for the training, test, and validation sets. The R^2-values for all the ANNs were high. Neural networks trained with the distal targets ($f > 0.8$) achieved the highest R^2 for both the training and test data sets and lowest rms error for all data sets. ANN2b had a slightly higher R^2-value (0.8677) than ANN2c (0.8630) on the validation set.

Table 3 summarizes data from the final set of trained neural networks. These networks were trained with the

Table 2 Summary Data Shown for Neural Networks Trained With Three Rotational Shoulder Angles and Two Translational Angles as Inputs Predicting the Elbow Angle as the Output. R^2 and Root Mean Squared Errors Shown for Train, Test, and Validation Sets

Name	Set	R^2	RMS
ANN2a	Train	0.8335	0.5639
	Test	0.8172	0.5908
	Valid	0.8223	0.5835
ANN2b	Train	0.8909	0.5076
	Test	0.8688	0.5568
	Valid	0.8677	0.5748
ANN2c	Train	0.9266	0.3614
	Test	0.9210	0.3757
	Valid	0.8630	0.4966

Table 3 Summary Data Shown for Neural Networks Trained With Three Rotational Shoulder Angles and Two Translational Angles as Inputs Predicting the Elbow Angle and Forearm Angle as the Output. R^2 and Root Mean Squared Errors Shown for Train, Test, and Validation Sets

Name	Output	Set	R^2	RMS
ANN3a	E_{FE}	Train	0.6222	0.8787
		Test	0.5486	0.7716
		Valid	0.6313	0.8390
	F_{PS}	Train	0.9184	0.2802
		Test	0.7748	0.4583
		Valid	0.8631	0.3569
ANN3b	E_{FE}	Train	0.6993	0.8738
		Test	0.6046	0.8085
		Valid	0.7068	0.8630
	F_{PS}	Train	0.9199	0.2794
		Test	0.7874	0.4389
		Valid	0.8821	0.3343
ANN3c	E_{FE}	Train	0.7244	0.6685
		Test	0.8281	0.4692
		Valid	0.8057	0.5812
	F_{PS}	Train	0.9297	0.2011
		Test	0.9279	0.2322
		Valid	0.9471	0.2119

three shoulder rotational angles and translational movements as the inputs and both the elbow flexion extension and forearm pronation/supination as the output. The R^2-values and rms errors are tabulated for each data set. ANN3c achieved the highest R^2 and lowest rms error for both inputs on all data sets and was the only ANN able to predict the outputs with strong correlations to the recorded outputs for all three data sets. The F_{PS} was consistently predicted accurately across all trained ANNs and data sets. The correlation for the predicted elbow output was relatively low for all data sets of ANN3a and on the training and test sets of ANN3b.

IV. DISCUSSION

From the results of ANN1a, -b, and -c, it is clear that neural networks using three shoulder rotational angles to predict the elbow angle during reaching in two-dimensions can be extended to adequately predict the elbow angle for reaching movements in a large three-dimensional extrapersonal space. Additionally, removing both weaker synergies and proximal targets improves the performance of the network.

Reaching in two dimensions did not require the additional shoulder translational movements because all targets were in the horizontal plane. Presenting targets in three dimensions and fixing the wrist forced the subject to make scapuloclavicular movements. Adding those shoulder translational movements as inputs to the neural networks resulted in an increase in performance.

As more and more degrees of freedom are added to both the input and the output of the neural network, it is often expected that the increased complexity will result in a decrease in performance. Adding the additional output of forearm pronation/supination did not significantly hinder the performance of a neural network on both outputs when an ANN was trained with just distal targets. The predictability of the network for the elbow angle decreased only slightly, while the R^2-value for the forearm pronation/supination output was extremely high ($R^2 = 0.95$) for ANN3c. As more targets were added to the primary data set, the performance on the E_{FE} output gradually decreased. Perhaps two separately trained networks for each output are required to reach a high level of performance on each output.

It should be noted that this experiment was highly constrained in terms of forearm movement. The forearm movement from the initial position to the target position was stereotyped in that the subject was always forced to grasp the handle in the same vertical orientation in space, but this actually requires a different anatomical pronation/supination posture depending on shoulder angles. These preliminary results suggest that there are useful synergies among the five shoulder inputs and the forearm angle, and that further studies are required to understand the full extent and potential clinical utility of this relationship.

In the study reported in this paper, we used Euler rotations to represent the joint movements in the ANN training data. This commonly used method of joint motion representation produces motion data that is easier to understand and interpret. But the trigonometric conversion from rotation matrices to Euler angles is prone to singularities in some areas of the workspace, which occur frequently in unconstrained 3-D reaching movements. During preprocessing of the data, we removed any singularities present in the data prior to neural network training. To prevent the singularity problem, we have also trained neural networks on the complete rotation matrices as inputs/outputs. There was no significant difference in the performance, but the nine-dimensional results are more difficult to visualize and interpret. In future studies, we plan to use quaternions to alleviate the problem of singularities.

Achieving a high level of offline neural network performance is encouraging, but these results do not provide any information about the tractability of these neural networks in a prosthetic system. In order to determine whether these predictive algorithms are actually stable and useful as a basis for real-time control, further studies are required to examine how these trained ANNs behave in real-time virtual reality simulations analogous to real-world prostheses and FES systems [11]. Informal tests of a subject's ability to use ANN3c to control a kinematic simulation of a prosthetic arm were encouraging. The subject was able to make stable and reasonably accurate reaches in the workspace with little training, but methods to

quantify such performance and learning remain to be implemented. Furthermore, it remains to be seen whether forcing the subject into a nonnatural reaching strategy by fixing the wrist movements has limited the tractability of these neural networks. Further studies need to be conducted to examine the significance of this constraint.

Eventually, we plan to embed these synergy models into controllers for FES and powered prosthetic limbs. In these systems, the residual shoulder movements would act as command signals to drive the movements of the distal limb or the prosthesis. Implanted and wearable sensors for the shoulder kinematics are under development [12]. We plan to use our virtual reality environment as a training tool with which a patient using stereogoggles can train to operate a simulation of their FES arm or transhumeral prosthetic. For FES patients, we plan to restore movement to the distal limb with injectable, wireless, FES devices called BIONs [13]. Command signals specifying desired joint angles would have to be converted into desired muscle activations according to an inverse model of musculoskeletal dynamics and any available sources of kinematic feedback. ■

REFERENCES

[1] M. D. Serruya, N. G. Hatsopoulos, L. Paninski, M. R. Fellows, and J. P. Donoghue, "Instant neural control of a movement signal," *Nature*, vol. 416, pp. 141–142, 2002.

[2] J. K. Chapin, K. A. Moxon, R. S. Markowitz, and M. A. Nicolelis, "Real-time control of a robot arm using simultaneously recorded neurons in the motor cortex," *Nature Neurosci.*, vol. 2, pp. 664–670, 1999.

[3] N. A. Bernstein, *The Coordination and Regulation of Movements*. Oxford, U.K.: Pergamon, 1967.

[4] K. L. Kilgore, P. H. Peckham, G. B. Thrope, M. W. Keith, and K. A. Gallaher-Stone, "Synthesis of hand grasp using functional neuromuscular stimulation," *IEEE Trans. Biomed. Eng*, vol. 36, pp. 761–770, 1989.

[5] K. L. Kilgore, P. H. Peckham, F. W. Montague, R. L. Hart, A. M. Bryden, M. W. Keith, H. Hoyen, and N. Bhadra, "An implanted upper extremity neuroprosthesis utilizing myoelectric control," in *Proc. 2nd Annual Int. Conf. IEEE EMBS*, 2005.

[6] D. B. Popovic and M. B. Popovic, "Tuning of a nonanalytic hierarchical control system for reaching with FES," *IEEE Trans. Biomed. Eng*, vol. 45, pp. 203–212, 1998.

[7] M. B. Popovic and D. B. Popovic, "Cloning biological synergies improved control of elbow neuroprostheses," *IEEE Eng. Med. Biol. Mag.*, vol. 20, pp. 74–81, 2001.

[8] S. D. Iftime, L. L. Egsgaard, and M. B. Popovic, "Automatic determination of synergies by radial basis function artificial neural networks for the control of a neural prosthesis," *IEEE Trans. Neural Syst. Rehabil. Eng.*, vol. 13, pp. 482–489, 2005.

[9] R. R. Kaliki, R. Davoodi, and G. E. Loeb, "Prediction of elbow trajectory from shoulder angles using neural networks," submitted for publication.

[10] S. E. Fahlman and C. Lebiere, "The cascade-correlation learning architecture," in *Advances in Neural Information Processing Systems*, vol. 2, D. S. Touretzky, Ed. San Mateo, CA: Morgan Kaufmann, 1990, pp. 524–532.

[11] M. Hauschild, R. Davoodi, and G. E. Loeb, "A virtal reality environment for designing and fitting neural prosthetic limbs," *IEEE Trans. Rehabil. Eng.*, vol. 15, pp. 9–15, 2007.

[12] G. E. Loeb and R. Davoodi, "The functional reanimation of paralyzed limbs," *IEEE Eng. Med. Biol. Mag.*, vol. 24, pp. 45–51, 2005.

[13] W. Tan, Q. Zou, E. S. Kim, and G. E. Loeb, "Sensing human arm posture with implantable sensors," in *Proc. EMBS. Conf. 2004*, 2004, vol. 6, pp. 4290–4293.

ABOUT THE AUTHORS

Rahul R. Kaliki received the B.S. degree in biomedical engineering (premedical) from the University of California, San Diego, in 2004. He is currently pursuing the Ph.D. degree at the University of Southern California, Los Angeles.

He is studying the use of shoulder kinematics as a means to predict and control distal joint angles of the upper limb to restore functionality to transhumeral amputees and C5/C6 spinal cord injury patients. His research interests also include neural prosthetics, reanimation of paralyzed limbs, upper limb prostheses, and motor control.

Rahman Davoodi received the B.S. degree in mechanical engineering and the M.Sc. degree in biomechanical engineering from Sharif University of Technology, Tehran, Iran, and the Ph.D. degree in biomedical engineering from the University of Alberta, Edmonton, AB, Canada.

He is currently a Research Assistant Professor in the Department of Biomedical Engineering, University of Southern California, Los Angeles. His current research is focused on the use of neural prostheses to restore normal daily activities such as standing, walking, reaching, and grasping to the paralyzed and amputee patients. He has developed machine-learning control techniques to enable coordinated man–machine interactions in these neural prosthetic systems. He has also developed several publicly available software tools to enable other researchers and engineers to easily model, simulate, and virtually prototype complex neural prosthetic systems for the paralyzed and amputee patients.

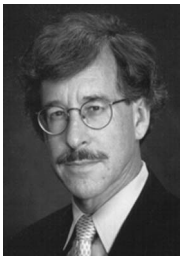

Gerald E. Loeb (Member, IEEE) received the B.A. and M.D. degrees from The Johns Hopkins University, Baltimore, MD, in 1969 and 1972, respectively.

He completed one year of surgical residency at the University of Arizona before joining the Laboratory of Neural Control, National Institutes of Health (NIH) (1973–1988). He was a Professor of physiology and biomedical engineering at Queen's University, Kingston, ON, Canada (1988–1999). He is now a Professor of biomedical engineering and neurology and Director of the Medical Device Development Facility, A. E. Mann Institute for Biomedical Engineering, University of Southern California, Los Angeles. He was one of the original developers of the cochlear implant to restore hearing to the deaf and was Chief Scientist for Advanced Bionics Corp. (1994–1999), manufacturers of the Clarion cochlear implant. He has received 43 issued U.S. patents and is the author of more than 200 scientific papers. Most of his current research is directed toward neural prosthetics to reanimate paralyzed muscles and limbs using a new technology that he and his collaborators developed called BIONs. This work is supported by an NIH Bioengineering Research Partnership and is one of the testbeds in the National Science Foundation's Engineering Research Center on Biomimetic MicroElectronic Systems, for which he is Deputy Director. These clinical applications build on his long-standing basic research into the properties and natural activities of muscles, motoneurons, proprioceptors, and spinal reflexes.

Prof. Loeb is a Fellow of the American Institute of Medical and Biological Engineers.